

Probabilistic Survival Analysis by Approximate Bayesian Inference of Neural Networks

Christian Marius Lillelund¹, Martin Magris² and Christian Fischer Pedersen¹

Abstract—Predicting future events always comes with uncertainty, but traditional non-probabilistic methods cannot distinguish certain from uncertain predictions. In survival analysis, probabilistic methods applied to state-of-the-art solutions in the healthcare and biomedical field are still novel, and their implications have not been fully evaluated. In this paper, we study the benefits of modeling uncertainty in deep neural networks for survival analysis with a focus on prediction and calibration performance. For this, we present a Bayesian deep learning framework that consists of three probabilistic network architectures, which we train by optimizing the Cox partial likelihood and combining input-dependent aleatoric uncertainty together with epistemic uncertainty. This enables us to provide uncertainty estimates as credible intervals when predicting the survival curve or as a probability density function over the predicted median survival times. For our empirical analyses, we evaluated our proposed method on four benchmark datasets and found that our method demonstrates prediction performance comparable to the state-of-the-art based on the concordance index and outperforms all other Cox-based approaches in terms of the mean absolute error. Our work explicitly compares the extent to which different Bayesian approximation techniques differ from each other and improves the prediction over traditional non-probabilistic alternatives.

Index Terms—Machine learning, Bayesian neural networks, survival analysis, Cox Proportional-Hazards, uncertainty estimation.

I. INTRODUCTION

Uncertainties appear regularly in many scenarios, from medical diagnoses and treatment recommendations to sports games and weather forecasting. With the adoption of machine learning algorithms and especially deep learning to guide the way we make decisions, it becomes increasingly important to assess whether we should trust the predictions made by such systems [1]. This is particularly true in safety-critical domains, such as healthcare, where confidence in a certain prognostic outcome can have life-changing implications. Machine learning algorithms often make predictions that are subject to noise or inference errors [2], which motivates the

use of models that can provide uncertainty estimates and a level of confidence in their predictions. In this context, we refer to *aleatoric* uncertainty, due to the inherent noise in the data [3], e.g., sampling noise, occlusions, or lack of quality features, and *epistemic* uncertainty, due to lack of knowledge in the model, inversely proportional to the amount of training data [4]. Aleatoric uncertainty can be further categorized into homoscedastic uncertainty, assuming constant conditional variance across inputs, and heteroscedastic uncertainty, where the variance depends on the inputs to the model [5].

Survival analysis plays an important role in disease understanding and prognosis, and medical researchers use survival models to assess the importance of prognostic variables in outcomes such as death or cancer remission. The Cox proportional hazards model (CoxPH) is an established semiparametric model for survival analysis [6]. The model assumes a linear log-risk function of an individual's covariates, which may be too simplistic in real applications [7]. To this end, neural networks (NNs) have shown promising results, especially when the number of observations and covariates is large [8]–[12]. The prevalent approach in these works is to optimize the Cox partial likelihood to provide a point estimation of the model parameters: this offers good predictive performance in areas with a lot of data, but can easily become biased in small datasets and give overly confident predictions [2]. To address these shortcomings, Bayesian neural networks (BNNs) have been proposed for survival analysis, using pseudo-probabilities [11], the aforementioned CoxPH model [13], [14], or Multi-Task Logistic Regression (MTLR) [14], [15].

In this work, we propose three probabilistic architectures for survival analysis: Spectral-normalized Neural Gaussian Process (SNGP), Variational Inference (VI), and Monte Carlo Dropout (MCD). We provide a thorough evaluation of their performance in terms of prediction and calibration, and compare them to established literature benchmarks. The use of VI to train BNNs for survival analysis is popular in the literature [11], [14], [15], but requires doubling the number of network parameters. This motivates the use of variational approximation techniques to Bayesian uncertainty estimation, but also mandates an empirical evaluation to check if the approximate predictive distribution keeps the qualitative features of the exact distribution. A preliminary version of this work has been reported in [13]. The source code is available on GitHub¹.

This work was supported by the PRECISE project (<http://www.aal-europe.eu/projects/precise/>) under Grant Agreement No. AAL-2021-8-90-CP by the European AAL Association.

¹The authors are with the Department of Electrical and Computer Engineering, Aarhus University, Finlandsgade 22, 8200 Aarhus N, Denmark. Emails: {cl, cfp}@ece.au.dk. ²The author is with the Dipartimento di Scienze Economiche, Aziendali, Matematiche e Statistiche, Università degli studi di Trieste, Via A. Valerio 4/1, 34127 Trieste, Italy. Email: martin.magris@deams.units.it

¹<https://github.com/thecml/baysurv>

II. RELATED WORK

A. Uncertainty estimation in deep learning

Although Deep Neural Networks (DNNs) have become attractive in healthcare and biomedical applications because of their high predictive performance, their application in safety-critical systems remains limited. This is mainly due to the lack of expressiveness and transparency of a deep neural network [16], their inability to distinguish between in-domain and out-of-domain samples [17], sensitivity to domain shifts [18], and their inability to provide reliable uncertainty estimates [2], [19]. Conventional maximum likelihood estimation, often used in traditional deep learning networks to estimate model parameters, offers good predictive performance in areas with abundant data, but is easily biased in small datasets delivering overconfident estimates [2]. In regions of the input space where there are no samples, the ordinary neural network fits a particular function, although there are many possible extrapolations of the training data. Thus Bayesian models have historically been adopted to bridge this gap, as they can express uncertainty about their predictions and provide implicit regularization. A Bayesian model trained by maximum a posterior (MAP) averages predictions over a posterior distribution of the parameters: where there are no data, the confidence intervals diverge, reflecting that there are many extrapolations [20]. Bayesian methods have been frequently used for the joint modeling of time-to-event data in the healthcare field [21]–[23], but it is not easy to determine its convergence and using the output of a Markov Chain Monte Carlo (MCMC) algorithm that has not converged can lead to incorrect inferences [24], and MCMC also suffers from long training times [24]. To leverage the benefits that DNNs provide in terms of performance and, at the same time, obtain reliable uncertainty estimates, researchers have proposed probabilistic Bayesian Neural Networks (BNNs). BNNs are artificial NNs trained using Bayesian inference [4], e.g., Variational Inference (VI) [25], to infer a posterior probability distribution over the network parameters. Once the posterior distribution over the weights has been estimated, the prediction of the output y^* for new input data x^* can be obtained by marginalizing the posterior distribution over the parameters. Variational methods approximate the true posterior distribution of the parameters with an approximate one of a tractable parametric form by optimizing the Kullback-Leibler (KL) divergence between the two. However, this often comes with a high computational cost, for which reason different approximate schemes have been proposed, e.g., Monte-Carlo Dropout (MCD) [2] and Spectral-normalized Neural Gaussian Process (SNGP) [26]. MCD makes a Bayesian VI approximation on the posterior of a general underlying deep Gaussian process model. This is done by introducing stochastic dropout layers that are turned off at test time to obtain samples from the VI approximate posterior (stochastic forward passes). MCD can provide cheap uncertainty estimation without long training times or diminished predictive accuracy [2], but does not provide an actual posterior, and the quality of its uncertainty estimates is closely coupled to the choice of parameters [27]–[30], e.g., the number of hidden layers and the dropout rate [31].

B. Uncertainty estimation in deep survival models

Ibrahim et al. provided a comprehensive review of Bayesian methods for time-to-event analysis in [32], later adopted by Alvares et al. using MCMC [33]. However, one of the main problems with using MCMC is the long training times and convergence issues in large-scale datasets [24], thus more recently approaches that factorize the likelihood over subsamples of the data have been proposed [34], [35]. By adopting the CoxPH model [6], Katzman et al. proposed DeepSurv, a multilayer perceptron (MLP) that optimizes the Cox partial likelihood using stochastic gradient descent (SGD) [9]. In 2021, Nagpal et al. proposed Deep Survival Machines (DSM), a fully-parametric MLP that can estimate the conditional survival distribution as a mixture of primitive distributions [36]. The parameters of the network are estimated by optimizing the evidence lower bound (ELBO), and the network output is subsequently passed through a nonlinear activation function to estimate the survival distribution primitives. Neural networks have shown solid performance in survival analysis motivating Bayesian methods for survival analysis in deep learning.

Loya et al. proposed a Bayesian extension of the MTLR framework that can capture patient-specific survival uncertainties [15]. MTLR was originally proposed by Yu et al. as a remedy to the assumption of temporal consistency of relative risk between two patients [37]. MTLR uses multitask regression and joint likelihood minimization to model log-risk in a given time interval as a linear combination of the covariates. Loya et al. adopted this structure using a BNN with an element-wise structure (the first and second layers must have the same number of neurons) with feature selection in mind. Using VI to learn the posterior distribution of the model weights and drawing samples from the predictive distribution, their model easily beats traditional CoxPH and MTLR in prediction accuracy while providing empirical confidence bounds on the predicted survival probability.

Qi et al. adopted the CoxPH and MTLR framework side by side to formulate a BNN for survival analysis [14]. The authors investigate how to select an appropriate prior distribution on the model weights when building the network, and how this can enforce sparsity for later feature selection. They also proposed a novel framework for estimating individual survival distributions (ISDs) with credible intervals and coverage guarantees around the survival curve, thus communicating the underlying uncertainty of the model weights. Their work is indeed applicable as a decision support system, as their survival curves are specific to an individual patient, not just population averages for a large group of patients.

Lillelund et al. showed that MCD can provide good predictive results in survival models, while being significantly faster to train than VI [13]. Using the CoxPH framework, they quantified epistemic and aleatoric uncertainty by replacing the network's weights with a distribution and sampling the network's outputs from a Gaussian. The results demonstrate that aleatoric and epistemic uncertainty can be included in a deep survival model at no additional cost, except the increase in training times.

III. MATERIALS AND METHODS

A. Survival analysis

Survival analysis is a regression aimed at modeling the time of a certain event. Such an event can be either observed or not, i.e., censored (e.g., due to the termination of the study). Let $\mathcal{D} = \{(t_i, \delta_i, \mathbf{x}_i)\}_{i=1}^N$ be the data for the i th record (individual), where t_i denotes the observed event time, δ_i is a binary event indicator (the event occurred/not occurred) and $\mathbf{x}_i \in \mathbb{R}^d$ is a d -dimensional vector of features (covariates). Moreover, let c_i denote the censoring time and e_i denote the event time for the i th record, thus $t_i = e_i$ if $\delta_i = 1$ or $t_i = c_i$ if $\delta_i = 0$. Survival analysis models the survival probability $S(t) = \Pr(T > t) = 1 - \Pr(t \leq T)$, that is, the probability that a certain event occurs at time T later than t . Let t_k denote some measurement time on some discretized event horizon of K bins, $[t_0, t_1, t_2, \dots, t_K]$, then at $t_k = 0$, the survival function $S(t_k)$ is one and monotonically decreases for $t_k > 0$, so that the probability of surviving indefinitely is zero. In the absence of censored observations, $S(t_k)$ corresponds to the fraction of survivors at time t_k . We define the hazard function as:

$$h(t) = \lim_{\Delta t \rightarrow 0} \Pr(t < T \leq t + \Delta t | T > t) / \Delta t \quad (1)$$

which provides the instantaneous failure *rate* at given time instant t , conditional on surviving t [38, Ch. 11]. The hazard function and the survival function are connected through $h(t) = f(t)/S(t)$, with $f(t)$ being the probability density of T , i.e. $f(t) := \lim_{\Delta t \rightarrow 0} \Pr(t < T \leq t + \Delta t) / \Delta t$, the instantaneous (unconditional) rate of failure at t . The functions $S(t)$, $h(t)$, $f(t)$, thus summarize different probabilistic aspects of the random variable T , related with each other.

B. The Cox Proportional Hazard model

The Cox proportional hazards model (CoxPH) is a standard approach for survival analysis [6]. By adopting a multiplicative form for the contribution of several covariates to each individual's survival time, the CoxPH model is a powerful yet simple tool for assessing the simultaneous effect that different covariates have on survival times. The conditional individual hazard function assumed by the CoxPH model is $h(t|\mathbf{x}_i) = h_0(t) \exp(f(\boldsymbol{\omega}, \mathbf{x}_i))$, where $h_0(t)$ stands for the baseline hazard at time t , $f(\boldsymbol{\omega}, \mathbf{x}_i)$ is referred to as risk score, and f is a linear function in the parameters [6]. Even if $h_0(t)$ remains unknown, it is possible to estimate $\hat{\boldsymbol{\omega}}$ independently in the exponential part, with estimated hazards that satisfy the non-negative constraint. The standard maximum likelihood estimation procedure for $\hat{\boldsymbol{\omega}}$ optimizes the partial log-likelihood:

$$\begin{aligned} \log p(\mathcal{D}|\boldsymbol{\omega}) &= \sum_{i:\delta_i=1} \log \frac{h(y_i|\mathbf{x}_i)}{\sum_{j:T_j \geq T_i} h(y_i|\mathbf{x}_j)}, \\ &= \sum_{i:\delta_i=1} f(\boldsymbol{\omega}, \mathbf{x}_i) - \sum_{j:T_j \geq T_i} f(\boldsymbol{\omega}, \mathbf{x}_j). \end{aligned} \quad (2)$$

Among the available estimators for $h_0(t)$, leading to the estimation of the survival function as $\hat{S}(t) = \hat{S}_0(t)^{\exp(\mathbf{x}_i \hat{\boldsymbol{\omega}})}$, with $\hat{S}_0(t) = \exp(-\int_0^t \hat{h}_0(u) du)$. The Kaplan-Meier nonparametric approach is the standard one [39].

C. Uncertainty in Bayesian Deep Learning

A Bayesian Neural Network (BNN) is a neural network estimated with Bayesian inference. In this paper, we discuss the use of BNN in the context of survival analysis.

Variational inference (VI): Let \mathcal{D} denote the data, $p(\mathcal{D}|\boldsymbol{\omega})$ the likelihood, and the prior distribution on the parameter be denoted by $\boldsymbol{\omega}$ as $p(\boldsymbol{\omega})$. The object of interest in Bayesian inference is the posterior distribution $p(\boldsymbol{\omega}|\mathcal{D}) = p(\mathcal{D}|\boldsymbol{\omega})p(\boldsymbol{\omega})/p(\mathcal{D})$. To obtain the distribution of the response \mathbf{y}^* for a new data sample \mathbf{x}^* the so-called posterior distribution is obtained as $p(\mathbf{y}^*|\mathbf{x}^*) = \int_{\Theta} p(\mathbf{y}^*|\mathbf{x}^*, \boldsymbol{\omega})p(\boldsymbol{\omega}|\mathcal{D})d\boldsymbol{\omega}$.

In general, determining the posterior is not an easy task, as the model evidence $p(\mathcal{D})$ corresponds to an intractable integral. When the dimensionality of the problem is high, the use of sampling methods is prohibitive, and Variational Inference (VI) constitutes an attractive alternative. In VI the true-but-unknown posterior distribution is approximated with a variational distribution $q(\boldsymbol{\omega})$ of a tractable parametric form, whose (variational) parameter is denoted by ζ . Typically this corresponds to a multivariate Gaussian with mean $\boldsymbol{\mu}$ and covariance matrix $\boldsymbol{\Sigma}$, thus $\zeta = [\boldsymbol{\mu}; \text{vec } \boldsymbol{\Sigma}]$. VI achieves the best variational approximation to $p(\boldsymbol{\omega}|\mathcal{D})$ by minimizing the KL divergence from $q(\boldsymbol{\omega})$ to $p(\boldsymbol{\omega}|\mathcal{D})$, i.e., determines the variational parameter ζ^* by minimizing:

$$\begin{aligned} \text{KL}(q(\boldsymbol{\omega})||p(\boldsymbol{\omega}|\mathcal{D})) &:= \\ &- \int q(\boldsymbol{\omega}) \log p(\mathcal{D}|\boldsymbol{\omega})d\boldsymbol{\omega} + \text{KL}(q(\boldsymbol{\omega})||p(\boldsymbol{\omega})), \end{aligned} \quad (3)$$

for which several algorithms have been developed in the last decade [4].

Monte-Carlo Dropout (MCD): [2] and [40] provide a formal connection between Monte Carlo Dropout (MCD) and BNNs. Here, we discuss the major breakthrough for the relevant noncategorical case for the \mathbf{y} s. Consider a deep Gaussian Process (GP) with covariance function of the form:

$$\mathbf{K}(\mathbf{x}, \mathbf{y}) = \int p(\mathbf{w})p(b)\sigma(\mathbf{w}^\top \mathbf{x} + b)\sigma(\mathbf{w}^\top \mathbf{y} + b)d\mathbf{w}db, \quad (4)$$

where \mathbf{W}_i the weight matrix of dimension $K_i \times K_{i-1}$ for each layer $i = 1, \dots, L$ and \mathbf{b}_i the corresponding bias vectors. We use $\boldsymbol{\omega} = \{\mathbf{W}_i\}_{i=1}^L$, where each row of \mathbf{W}_i distributed according to a standard multivariate normal distribution $p(\mathbf{w}) = \mathcal{N}(\mathbf{w}; \mathbf{0}, \mathbf{I})$. Be $\sigma(\cdot)$ a general non-linear activation function and $p(b)$ some distribution on the elements of \mathbf{b}_i . Given some precision parameter $\tau > 0$, the predictive distribution of the deep GS is:

$$p(\mathbf{y}|\mathbf{x}) = \int p(\mathbf{y}|\mathbf{x}, \boldsymbol{\omega})p(\boldsymbol{\omega}|\mathcal{D})d\boldsymbol{\omega} \quad (5)$$

with

$$p(\mathbf{y}|\mathbf{x}, \boldsymbol{\omega}) = \mathcal{N}(\mathbf{y}; \hat{\mathbf{y}}(\mathbf{x}, \boldsymbol{\omega}), \tau^{-1}\mathbf{I}). \quad (6)$$

For the intractable posterior $p(\boldsymbol{\omega}|\mathcal{D})$, adopt a variational approximation $q(\boldsymbol{\omega})$ defined as:

$$\mathbf{W}_i = \mathbf{M} \cdot \text{diag}([z_{i,j}]_{j=1}^{K_i}), \quad (7)$$

$$z_{i,j} \sim \text{Bernoulli}(p_i), i = 1, \dots, L, j = 1, \dots, K_{i-1}, \quad (8)$$

where \mathbf{M}_i are the variational parameters and p_i some given probabilities. [2] shows that minimizing the KL divergence between the variational posterior $q(\omega)$ and the actual posterior of the deep GP is equivalent to optimizing with dropout the following objective:

$$\mathcal{L}_{\text{MCD}} = \frac{1}{N} \sum_{i=1}^N E(\mathbf{y}_i, \hat{\mathbf{y}}_i) + \lambda \sum_{i=1}^N (\|\mathbf{W}_i\|_2^2 + \|\mathbf{b}_i\|_2^2). \quad (9)$$

L is a standard non-probabilistic optimization objective, using the L_2 regularization and tuning parameter λ and the Euclidean square loss $E(\cdot, \cdot)$. Dropout means that for every input data and every unit in each layer, a Bernoulli variable is sampled with probability p_i , and a unit is dropped if the corresponding binary variable is 0. The probability $1 - p$ of dropping a unit is usually called the dropout rate. Therefore, a DNN, with dropout applied at every layer, is equivalent to a Monte Carlo approximation to the probabilistic deep GP; i.e., it minimizes the KL divergence between the variational distribution and the posterior of the deep Gaussian process modeling the distribution over the space of distributions that can have generated the data. It is straightforward to approximate the predictive distribution as follows:

$$p(\mathbf{y}^* | \mathbf{x}^*) = p(\mathbf{y}^* | \mathbf{x}^*, \omega) q(\omega), \quad (10)$$

$$q(\omega) = \text{Bernoulli}(z_1) \cdots \text{Bernoulli}(z_L), \quad (11)$$

$$p(\mathbf{y}^* | \mathbf{x}^*, \omega) = \mathcal{N}(\mathbf{y}^*; \hat{\mathbf{y}}^*(\mathbf{x}^*, z_1, \dots, z_L), \tau^{-1} \mathbf{I}), \quad (12)$$

and, e.g., its mean through MC sampling:

$$\mathbb{E}_{p(\mathbf{y}^* | \mathbf{x}^*)} \approx \frac{1}{S} \sum_{s=1}^S \hat{\mathbf{y}}^*(\mathbf{x}^*, \hat{z}_{1,s}, \dots, \hat{z}_{L,s}), \quad (13)$$

$$\hat{z}_{i,s} \sim \text{Bernoulli}(p_i). \quad (14)$$

The practical simplicity of MCD makes it an attractive and widely adopted baseline for comparison with alternative Bayesian approaches. However, within neural network applications in survival analysis, the use of MCD for uncertainty quantification is very limited [13].

Spectral-normalized Neural Gaussian Process: The Spectral-normalized Neural Gaussian Process (SNGP) network [41] is a simple approach for improving the quality of uncertainty modeling in a deep neural network whilst preserving its overall predictive accuracy. Over a deep residual network, SNGP applies spectral normalization to the hidden layers and replaces the dense output layer with a Gaussian process layer. Compared to MCD, SNGP works for a wide range of state-of-the-art residual-based architectures. Furthermore, it does not rely on ensemble averaging. Therefore, SNGP has a similar level of latency as a deterministic network (besides requiring a covariance reinitialization of low complexity at each iteration), scaling easily to large dimensions and lengthy

datasets. Even though the predictive distribution relies on the Laplace approximation, which is different from the one of an actual Gaussian process, the SNGP architecture has a strong out-of-sample detection performance because of its distance-awareness property.

D. Our proposed method

For the purpose of comparability in the results, consistency in the hyperparameters, and evaluation fairness, we propose a multilayer perceptron (MLP) backbone network architecture. An MLP is a fully connected feedforward NN; the number of hidden layers L and neurons are hyperparameters tuned based on the data, see, e.g., [4]. The adoption of an MLP is aligned with the literature, as capable of providing solid predictive performance [9], [36], [42]. The proposed architecture is depicted in Fig. 1. There are three probabilistic configurations:

- i Probabilistic approach trained with SNGP. The predictive (epistemic) uncertainty of SNGP is computed using the Laplace approximation and allows estimating the predictive uncertainty on a per-sample basis without MC sampling. Given a batch input $\{\mathbf{x}_1, \mathbf{x}_2, \dots, \mathbf{x}_N\}$, the GP layer returns predictions $\{y_1, y_2, \dots, y_N\}$ and a covariance matrix $\Sigma^{N \times N}$, i.e., the predictive covariance matrix of the batch logits. The model is optimized according to the likelihood in Eq. (2). See Fig. 1c.
- ii Probabilistic approach trained with VI, learning the variational approximation by optimizing Eq. (3), where weights and biases are treated as random variables. The output nodes provide the mean and standard deviation of the output \hat{y}_i as a Gaussian draw, i.e., $\hat{y}_i \sim \mathcal{N}(\mu_{\mathbf{x}_i}, \sigma_{\mathbf{x}_i})$ for a d -dimensional sample \mathbf{x}_i . The Bayesian framework captures the epistemic uncertainty in the model, and sampling the output from a Gaussian captures the heteroscedastic aleatoric uncertainty. See Fig. 1a.
- iii Probabilistic approach trained with MCD. We set dropout rates to $p = \{0.1, 0.2, 0.5\}$, capturing both epistemic and heteroscedastic aleatoric uncertainty. This corresponds to a deterministic MLP, but with MC dropout at test-inference time and optimized according to the likelihood function in Eq. 2, and two output nodes corresponding to the mean and variance of the predictive Gaussian distribution, from which the y_i s are drawn conditionally on \mathbf{x}_i and the random network configuration at each epoch due to the random deactivation of some of the nodes. See Fig. 1b.

IV. EXPERIMENTS AND RESULTS

A. Setup

We use four datasets to evaluate our method. The Molecular Taxonomy of Breast Cancer International Consortium (METABRIC) dataset contains gene and protein expression profiles used to identify subgroups of breast cancer [43]. This was used to guide physicians in treatment recommendation for cancer patients. We obtain the dataset from the DeepSurv [9] paper, where the rows with missing values have been dropped. It has 1904 observations and 9 features with a censoring rate of 42%. The U.S. Surveillance, Epidemiology, and End Results

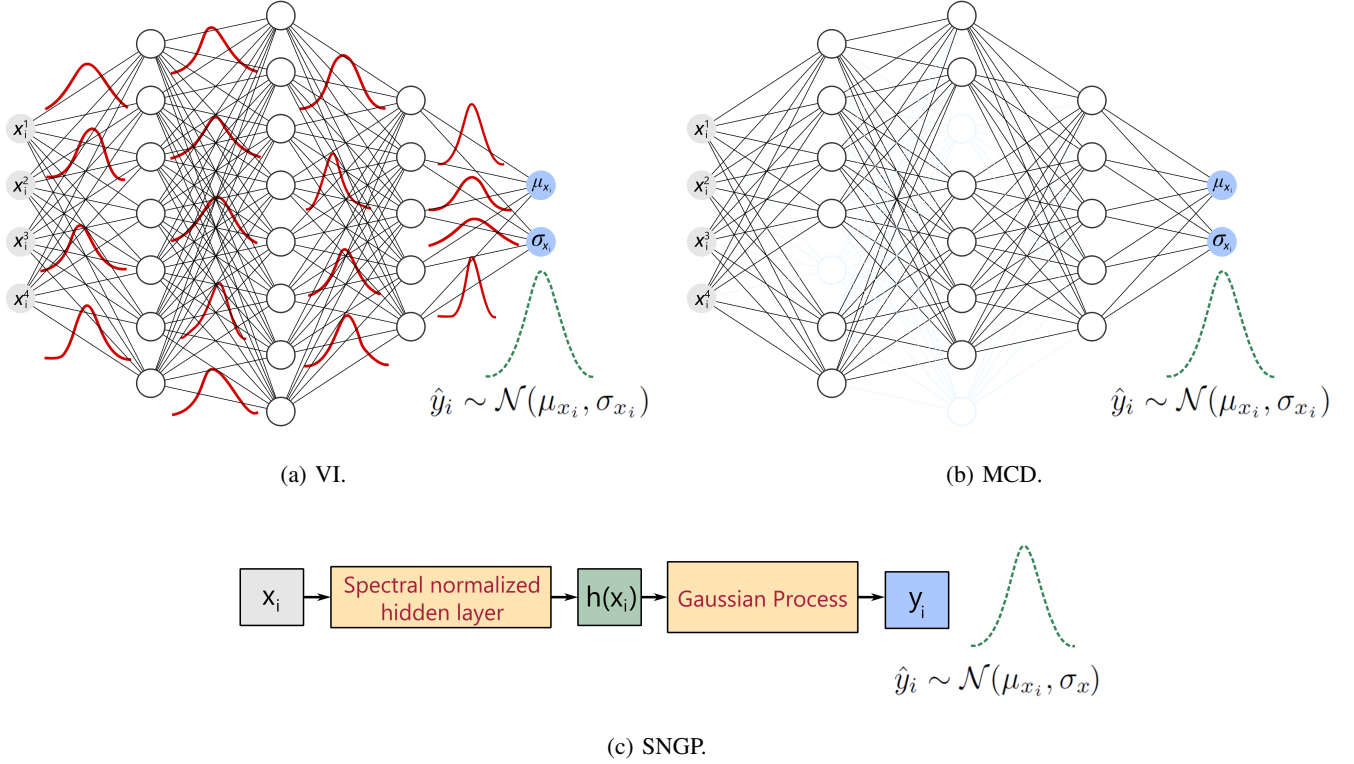


Fig. 1: Network architectures. (a): fully connected MLP network with three hidden layers trained with VI, with x_i being a four-dimensional vector. (b): MLP network with three hidden layers trained with MCD. Transparent objects emphasize the random activation of the nodes under MCD. (c): fully connected MLP network using the SNGP technique, with spectral normalized hidden layers and the output computed from a Gaussian Process layer.

(SEER) dataset contains survival times for cancer patients [44], specifically females with infiltrating duct and lobular carcinoma breast cancer diagnosed between 2006 and 2010. The dataset has 4024 observations and a censoring rate of 85%. The Study to Understand Prognoses Preferences Outcomes and Risks of Treatment (SUPPORT) dataset is a large study that tracks survival time of hospitalized adults [45]. We obtain the dataset from the DeepSurv [9] paper, where the rows with missing values have been dropped. The dataset has 8873 observations and 14 features with a censoring rate of 32%. MIMIC-IV is a large electronic health record dataset that covers 40,000 patients admitted to intensive care units (ICUs) at the Beth Israel Deaconess Medical Center in the United States between 2008 and 2019 [46]. The dataset includes patient demographics, clinical measurements such as vital signs and imaging reports, medications, and diagnoses, recorded during a patient’s stay in the ICU. The dataset also includes the survival time for patients who survived a minimum of 24 hours after ICU admission, with their date of death obtained from hospital or state records. We followed the instructions by Qi et al. [14] to create the dataset. It has 38520 observations and 91 features with a censoring rate of 67%. After imputing missing values by sample mean for real-valued covariates or mode for categorical covariates, we apply *az*-score data normalization and use one-hot encoding for categorical covariates. We split the data into train, validation and test sets by 70%, 10%, and 20% using a stratified procedure, as proposed by [14]. The

stratification ensures that the event times and censoring rates are consistent across the three sets.

For the purpose of comparability in the results, we implement the traditional CoxPH model [6], a CoxPH model with weight regularization [47], a CoxPH model using gradient boosting [48], Random Survival Forest [49], two non-Bayesian neural networks [36], [50], and two recent Bayesian neural networks based on the CoxPH and MTLR framework, respectively [14]. For all datasets and models, we use Bayesian optimization [51] to tune the hyperparameters over ten iterations in the validation set. This includes the number of iterations, the batch size and network architecture, if applicable, and is done solely on the 10% validation set. We use the hyperparameters leading to the highest average concordance index (Antolini’s) to configure the final models. The CoxPH-based models utilize the entire dataset size when training, given the nature of the partial likelihood, whereas the neural networks load stochastic subsets of the training set as minibatches. Additionally, we use the early stopping technique, where the training process halts if the likelihood loss of the model stops improving on the validation dataset, for all neural network-based models. See Appendix II for more details on hyperparameter optimization.

We adopt several evaluation metrics to assess the predictive and calibration performance of our baseline MLP model, its probabilistic variants, and literature benchmarks. To evaluate predictive performance, we report Antolini’s concordance index (CI) [52], the mean absolute error (MAE) using a hinge

loss [53], the MAE using pseudo-observations [53] and the Integrated Brier Score (IBS) [54]. To evaluate calibration performance, we report the Integrated Calibration Index (ICI) [55], Distribution Calibration (D-Cal) [56] and Coverage Calibration (C-Cal) [14]. See Appendix I for more details on performance metrics.

B. Prediction results

Table I shows the predictive performance of our baseline MLP and its probabilistic variants, and literature benchmarks on the test sets. For VI and MCD, the reported metrics are constructed based on predictive means over 100 posterior draws. The proposed neural network architectures were trained for 100 epochs using early stopping with five epochs of patience. Concerning the baseline MLP model and the SNGP, VI and MCD variants, on the smallest METABRIC dataset (see Tab. Ia), all probabilistic models report a higher concordance index (CI_{id}) and the MCD especially shows a significantly lower MAE (MAE_H and MAE_{PO}) than their baseline counterpart, thus modeling both aleatoric and epistemic uncertainty using VI or MCD improves predictive performance. In the mid-sized SEER dataset (see Tab. Ib), all probabilistic variants give approximately the same concordance index, but have a significantly lower MAE_H than the baseline. On the contrary, in the larger SUPPORT dataset (see Tab. Ic), the SNGP and Bayesian variants struggle to keep up with the baseline MLP in all comparable metrics, with only MCD ($p = 0.5$) outperforming both the baseline and its rival probabilistic models. In the large MIMIC-IV dataset (see Tab. Id), the effect of the different estimation approaches is reduced, and all measures are generally aligned with each other, although VI and MCD still have a slight edge when it comes to MAE_H . We observe that for all datasets, setting a dropout rate of $p = 0.5$ when using MCD to approximate the VI solution leads to better convergence and better predictive performance than the baseline MLP.

With respect to the existing models, MCD with $p = 0.5$ outperforms all other Cox-based models in terms of MAE_H , only surpassed by BNN-MTLR. We see a clear advantage in combining the MLP architecture with Bayesian approximation techniques to rank individuals at risk and predict the time to event via the survival function. These benefits are most apparent in small-sized datasets, as the Bayesian algorithms naturally incorporate a form of regularization (the prior) and hence are less prone to overfitting. As the size of the dataset increases, the effect of the prior diminishes, and the Bayesian solution approximates the frequentist one. Most importantly, adopting Bayesian methods does not deteriorate model performance in any of our experiments; rather, in many situations, it improves it. Concerning the large MIMIC-IV dataset, our MCD model with $p = 0.5$ outperforms all rival models in terms of concordance index (CI_{id}).

C. Calibration results

Table II shows the calibration performance of our baseline MLP and its SNGP, VI, and MCD, as well as variants and literature benchmarks on the test sets. Regarding the baseline

MLP model and its probabilistic variants, all models are D-calibrated on the small METABRIC dataset (see Tab. IIa), with the VI and MCD variants also being C-calibrated. We assess the agreement between predicted and observed survival probabilities using the ICI metric, i.e., the absolute difference between the calibration curve and the diagonal line of perfect calibration. We see that the MCD models improve on the baseline in terms of ICI and thus provide a better-calibrated survival curve. Using VI, despite being distribution and coverage calibrated, has a four-time higher ICI score than the MCD ($p = 0.5$) in the METABRIC dataset. In the mid-sized SEER dataset (see Tab. IIb), all proposed architectures are again properly distributed and coverage calibrated; however, we do observe a slight decrease in calibration performance in terms of ICI when adopting the VI and MCD methods, which is also evident in the lower p -values for D-Cal. In the SUPPORT dataset (see Tab. IIc), only the SNGP variant is statistically D-calibrated when compared to the other probabilistic approaches, but their ICI scores are not markedly higher than the baseline or the SNGP. We observe a similar trend in the large MIMIC-IV dataset (see Tab. IId), as none of the probabilistic methods are D-calibrated except the SNGP. Regarding the tight coupling between the quality of the MCD uncertainty estimates and the parameter choices, e.g., dropout layers, how many to use, and the choice of dropout rate, we conduct empirical experiments with various dropout rates to measure its effect. In terms of calibration performance, we do not see significant differences using either a low or high dropout rate; however, in the SEER, SUPPORT, and MIMIC-IV datasets, setting $p = 0.1$ does provide higher p -values for D-calibration.

With respect to the existing models, our SNGP and MCD variants and the BNN-Cox model are among those that give the lowest ICI scores on average, but do not necessarily provide D-calibrated survival curves. In the large MIMIC-IV dataset, neither the existing neural network models nor our proposed VI and MCD variants are D-calibrated, except for the BNN-MTLR model. The SNGP approach, comprising a deterministic MLP with the output computed from a Gaussian Process layer, is properly D-calibrated across all experimental datasets. It is important to rigorously assess multiple metrics to assess how calibrated a model truly is because each of them has a different goal and it may be use-case specific which type of calibration is needed. We note that all proposed models have been optimized according to the Cox partial likelihood, which optimizes for discriminative performance, not calibration performance. A method designed to maximize the Cox partial likelihood also ends up (approximately) maximizing the concordance index [58].

Figure 3 shows the calibration curves of the baseline and its probabilistic variants in the METABRIC dataset visually. We compare the survival models against the observed frequencies of event at four percentiles (25th, 50th, 75th, and 90th) of the survival time and create a smoothed calibration curve using a flexible spline regression model. The ranges of the predicted probabilities in the test set at the 90th percentile are as follows: 0.239 to 1 (MLP), 0.413 to 0.998 (SNGP), 0.208 to 0.973 (VI), 0.261 to 1 (MCD, $p = 0.1$), 0.086 to 1 (MCD, $p = 0.2$) and

TABLE I: Prediction performance on the METABRIC, SEER, SUPPORT and MIMIC-IV test sets. N : total sample size, C : pct. of censored data, d : number of covariates.

(a) METABRIC ($N = 1902$, $C = 42\%$, $d = 9$).					(b) SEER ($N = 4024$, $C = 85\%$, $d = 28$).				
Model	CI _{id} ↑	MAE _H ↓	MAE _{PO} ↓	IBS ↓	Model	CI _{id} ↑	MAE _H ↓	MAE _{PO} ↓	IBS ↓
CoxPH [6]	0.618	68.923	96.797	0.173	CoxPH [6]	0.723	100.849	196.898	0.083
CoxNet [47]	0.611	68.288	97.631	0.173	CoxNet [47]	0.721	95.253	197.066	0.083
CoxBoost [57]	0.638	69.976	102.745	0.187	CoxBoost [57]	0.689	106.635	232.204	0.092
RSF [49]	0.641	67.242	98.728	0.175	RSF [49]	0.682	102.062	206.41	0.086
DSM [36]	0.670	70.361	100.83	0.170	DSM [36]	0.699	153.84	413.543	0.088
DCM [50]	0.637	74.187	104.532	0.179	DCM [50]	0.713	108.464	223.397	0.082
BNN-Cox [14]	0.672	65.777	94.184	0.166	BNN-Cox [14]	0.716	95.184	202.151	0.081
BNN-MTLR [14]	0.655	59.027	89.387	0.163	BNN-MTLR [14]	0.702	48.166	201.856	0.085
This work:					This work:				
Baseline (MLP)	0.604	68.668	95.540	0.168	Baseline (MLP)	0.703	101.972	204.408	0.084
+ SNGP	0.631	67.378	93.434	0.166	+ SNGP	0.698	106.032	209.498	0.084
+ VI	0.634	63.776	91.843	0.168	+ VI	0.699	81.923	199.796	0.084
+ MCD ($p = 0.1$)	0.621	67.235	93.981	0.167	+ MCD ($p = 0.1$)	0.702	91.202	203.457	0.084
+ MCD ($p = 0.2$)	0.628	67.371	96.184	0.166	+ MCD ($p = 0.2$)	0.691	89.103	203.323	0.085
+ MCD ($p = 0.5$)	0.632	65.651	92.353	0.164	+ MCD ($p = 0.5$)	0.692	82.001	207.956	0.087

(c) SUPPORT ($N = 8873$, $C = 32\%$, $d = 14$).					(d) MIMIC-IV ($N = 38520$, $C = 67\%$, $d = 91$).				
Model	CI _{id} ↑	MAE _H ↓	MAE _{PO} ↓	IBS ↓	Model	CI _{id} ↑	MAE _H ↓	MAE _{PO} ↓	IBS ↓
CoxPH [6]	0.568	409.947	754.978	0.201	CoxPH [6]	0.726	257.364	286.516	0.174
CoxNet [47]	0.568	409.915	754.960	0.201	CoxNet [47]	0.727	255.802	283.951	0.174
CoxBoost [57]	0.612	366.928	721.443	0.190	CoxBoost [57]	0.656	263.836	297.763	0.194
RSF [49]	0.602	377.862	736.800	0.200	RSF [49]	0.694	260.668	293.247	0.188
DSM [36]	0.626	384.349	723.002	0.185	DSM [36]	0.727	259.110	280.361	0.180
DCM [50]	0.629	434.376	759.509	0.185	DCM [50]	0.742	257.801	286.580	0.174
BNN-Cox [14]	0.610	416.650	738.350	0.189	BNN-Cox [14]	0.743	256.007	288.814	0.169
BNN-MTLR [14]	0.606	369.060	707.679	0.186	BNN-MTLR [14]	0.744	250.605	278.710	0.167
This work:					This work:				
Baseline (MLP)	0.609	391.573	722.709	0.187	Baseline (MLP)	0.744	256.694	283.635	0.178
+ SNGP	0.610	397.877	726.725	0.184	+ SNGP	0.736	257.195	282.082	0.182
+ VI	0.531	414.133	768.599	0.208	+ VI	0.743	254.735	282.345	0.180
+ MCD ($p = 0.1$)	0.600	416.175	738.567	0.193	+ MCD ($p = 0.1$)	0.746	255.815	283.672	0.177
+ MCD ($p = 0.2$)	0.567	400.064	751.343	0.202	+ MCD ($p = 0.2$)	0.748	254.560	283.156	0.175
+ MCD ($p = 0.5$)	0.605	374.046	717.227	0.192	+ MCD ($p = 0.5$)	0.748	254.971	281.928	0.177

0.097 to 1 (MCD, $p = 0.5$). While the calibration curves for the MCD and SNGP variants are visually better than the VI, it is still difficult to determine from the plot alone which model is better calibrated at various survival times.

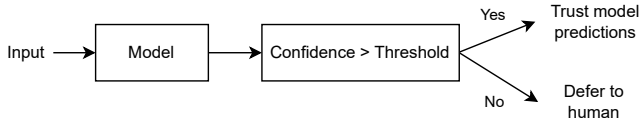


Fig. 2: Illustration of a workflow involving a model that is mindful of uncertainties. If the model prediction satisfies a confidence threshold, we trust it; otherwise, it is passed on to a human for additional evaluation.

D. Uncertainty estimation

We adopt the notion of credible intervals (CrIs) from [14]. CrIs in the Bayesian framework offer a way to quantify the uncertainty associated with a prediction. A credible interval is defined by two values, referred to as the lower and upper bounds, which enclose a certain percentage of the predictive distribution. The main difference between Bayesian CrIs and their frequentist counterpart, confidence intervals (CIs), is that

CrIs treat the parameter of interest as a random variable and the bounds as fixed values, while CIs treat the parameter of interest as a fixed value and the bounds as random variables. Figure 4 shows two ways in which uncertainty can be expressed along with a survival prediction for decision support purposes. For this, we selected a random sample from the METABRIC test set and drew 1000 samples from the predictive distribution of the model to estimate the survival curve. Although both MCD (upper panel) and VI (lower panel) agree on the median survival time, \hat{y}_t , the latter predicts a higher amount of variance around the survival curve and in the probability density function than the former. The width of the CrIs expresses the model's uncertainty, which is especially useful when making predictions about novel individuals (new data samples). Adopting an AI model that can express uncertainty about its predictions can help medical practitioners make tailor-made treatment plans with an extra level of risk assessment and understanding to it. This in turn can increase the level of trust and confidence that practitioners, patients and relatives put in the prediction. Non-probabilistic models cannot offer these advantages.

TABLE II: Calibration performance on the METABRIC, SEER, SUPPORT and MIMIC-IV test sets. D/C-Calibration and C-calibration are reported by a model's p -value according to a Pearson's χ^2 goodness-of-fit test. Calibrated models have p -values greater than 0.05, indicated by a Yes/No. A p -value close to one suggests good calibration. A p -value close to one suggests good calibration. C-calibration is only applicable for models that can predict credible regions (CrIs) [14]. N : total sample size, C : pct. of censored data, d : number of covariates.

(a) METABRIC ($N = 1902$, $C = 42\%$, $d = 9$).				(b) SEER ($N = 4024$, $C = 85\%$, $d = 28$).			
Model	ICI ↓	D-Cal ↑	C-Cal ↑	Model	ICI ↓	D-Cal ↑	C-Cal ↑
CoxPH [6]	0.022	0.959 (Yes)	-	CoxPH [6]	0.011	0.999 (Yes)	-
CoxNet [47]	0.011	0.977 (Yes)	-	CoxNet [47]	0.013	1.000 (Yes)	-
CoxBoost [57]	0.147	0.822 (Yes)	-	CoxBoost [57]	0.051	1.000 (Yes)	-
RSF [49]	0.047	0.530 (Yes)	-	RSF [49]	0.021	1.000 (Yes)	-
DSM [36]	0.025	0.017 (No)	-	DSM [36]	0.009	0.931 (Yes)	-
DCM [50]	0.066	0.160 (Yes)	-	DCM [50]	0.016	1.000 (Yes)	-
BNN-Cox [14]	0.017	0.101 (Yes)	0.812 (Yes)	BNN-Cox [14]	0.009	1.000 (Yes)	0.489 (Yes)
BNN-MTLR [14]	0.044	0.438 (Yes)	0.763 (Yes)	BNN-MTLR [14]	0.056	0.016 (No)	0.486 (Yes)
This work:				This work:			
Baseline (MLP)	0.040	0.853 (Yes)	-	Baseline (MLP)	0.009	1.000 (Yes)	-
+ SNGP	0.017	0.964 (Yes)	-	+ SNGP	0.011	1.000 (Yes)	-
+ VI	0.062	0.059 (Yes)	0.796 (Yes)	+ VI	0.027	0.678 (Yes)	0.487 (Yes)
+ MCD ($p = 0.1$)	0.017	0.735 (Yes)	0.849 (Yes)	+ MCD ($p = 0.1$)	0.013	0.989 (Yes)	0.487 (Yes)
+ MCD ($p = 0.2$)	0.020	0.689 (Yes)	0.857 (Yes)	+ MCD ($p = 0.2$)	0.014	0.983 (Yes)	0.487 (Yes)
+ MCD ($p = 0.5$)	0.017	0.760 (Yes)	0.865 (Yes)	+ MCD ($p = 0.5$)	0.037	0.841 (Yes)	0.486 (Yes)

(c) SUPPORT ($N = 8873$, $C = 32\%$, $d = 14$).				(d) MIMIC-IV ($N = 38520$, $C = 67\%$, $d = 91$).			
Model	ICI ↓	D-Cal ↑	C-Cal ↑	Model	ICI ↓	D-Cal ↑	C-Cal ↑
CoxPH [6]	0.059	0.983 (Yes)	-	CoxPH [6]	0.037	0.549 (Yes)	-
CoxNet [47]	0.059	0.983 (Yes)	-	CoxNet [47]	0.033	0.553 (Yes)	-
CoxBoost [57]	0.019	0.708 (Yes)	-	CoxBoost [57]	0.016	0.997 (Yes)	-
RSF [49]	0.022	0.532 (Yes)	-	RSF [49]	0.041	0.935 (Yes)	-
DSM [36]	0.065	0.000 (No)	-	DSM [36]	0.006	0.000 (No)	-
DCM [50]	0.090	0.904 (Yes)	-	DCM [50]	0.041	0.011 (No)	-
BNN-Cox [14]	0.073	0.096 (Yes)	0.952 (Yes)	BNN-Cox [14]	0.066	0.001 (No)	0.589 (Yes)
BNN-MTLR [14]	0.042	0.029 (No)	0.947 (Yes)	BNN-MTLR [14]	0.057	0.060 (Yes)	0.583 (Yes)
This work:				This work:			
Baseline (MLP)	0.069	0.229 (Yes)	-	Baseline (MLP)	0.026	0.068 (Yes)	-
+ SNGP	0.075	0.689 (Yes)	-	+ SNGP	0.015	0.230 (Yes)	-
+ VI	0.064	0.000 (No)	0.977 (Yes)	+ VI	0.096	0.000 (No)	0.583 (Yes)
+ MCD ($p = 0.1$)	0.077	0.000 (No)	0.938 (Yes)	+ MCD ($p = 0.1$)	0.034	0.014 (No)	0.600 (Yes)
+ MCD ($p = 0.2$)	0.061	0.000 (No)	0.979 (Yes)	+ MCD ($p = 0.2$)	0.038	0.013 (No)	0.596 (Yes)
+ MCD ($p = 0.5$)	0.050	0.000 (No)	0.956 (Yes)	+ MCD ($p = 0.5$)	0.036	0.008 (No)	0.597 (Yes)

V. CONCLUSION

Assessing uncertainty in high-risk domains, such as healthcare, is of utmost importance for boosting the point prediction that traditional approaches deliver. Figure 2 illustrates the workflow of using a model that can provide uncertainties along with its prediction. Given a confidence threshold, we can choose to trust its prediction or defer it to a human. This is the main advantage of using probabilistic methods, since traditional non-probabilistic methods cannot distinguish certain from uncertain predictions. In particular, in survival analysis, probabilistic methods applied to state-of-the-art solutions are very novel, and their implications are not extensively assessed. In this work, we have applied and evaluated three probabilistic architectures that allow to model and include aleatoric, epistemic, and both uncertainties for survival analysis. Over a wide set of traditional benchmark models, widely employed reference datasets, and existing models in the literature, we show the benefit of employing SNGP networks, Variational Inference (VI), and Monte Carlo Dropout (MCD) as effective solutions for modeling uncertainties in deep neural networks

for survival analysis. Supported by a number of tables, detailed analyses, and graphical illustrations, our main takeaways are as follows:

- The adoption of probabilistic techniques exhibits state-of-the-art predictive performance in real-world clinical datasets, and in particular, using MCD with a high dropout rate ($p = 0.5$) provides better survival estimates in terms of mean absolute error (MAE) than all benchmark models, except MTLR. Our empirical experiments have shown that adopting the Bayesian framework does not worsen predictive performance compared to deterministic models, but actually improves them in many scenarios.
- We find that in small-sized datasets, the goodness-of-fit test for D-calibration is easier satisfied for the Bayesian models compared to large-sized datasets. The baseline MLP and the probabilistic SNGP variant satisfy the assumption in all datasets, but introducing more degrees of freedom in the model and modeling heteroscedastic variance in the output, makes it easier to fail the hypothesis test. For example, the linear CoxPH model is

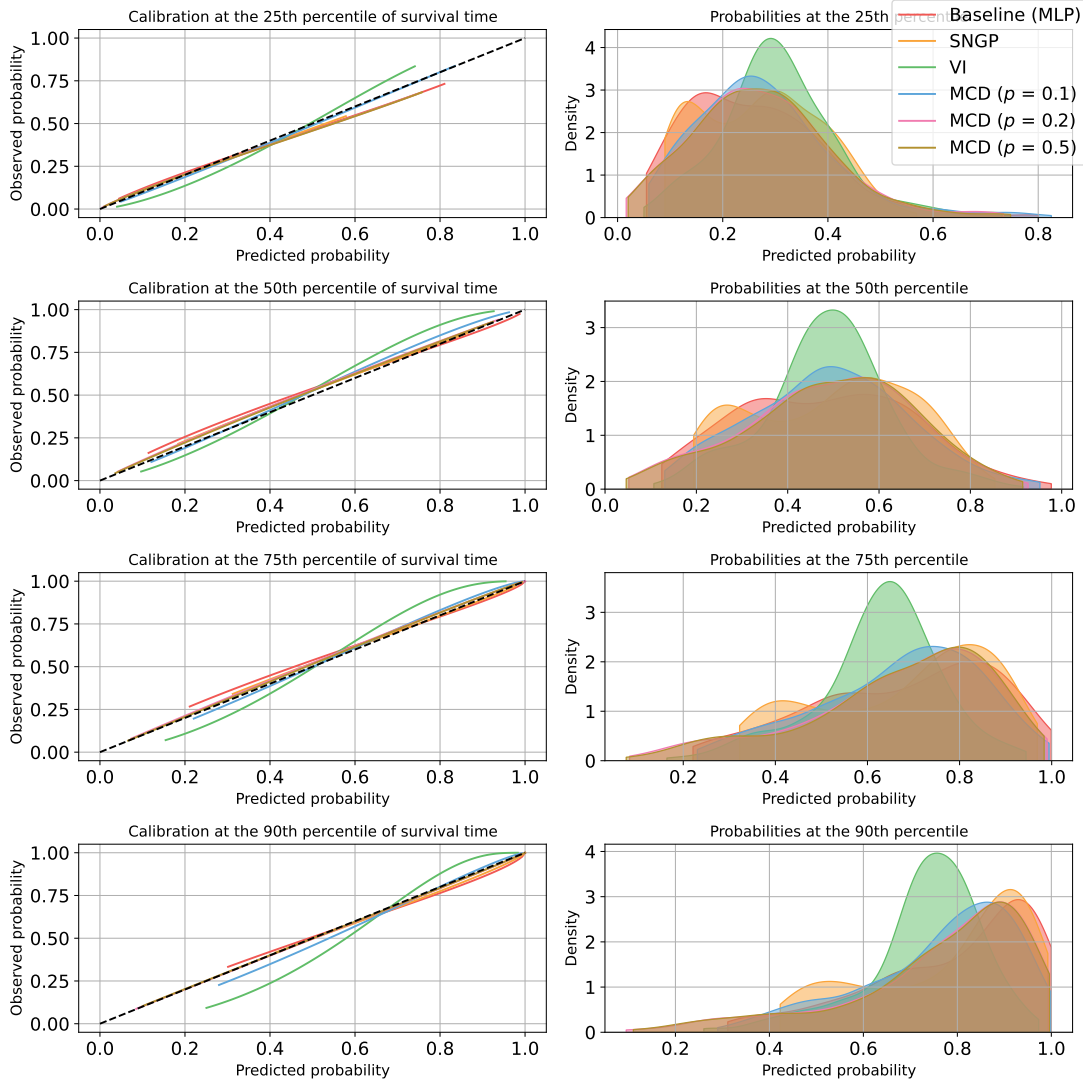


Fig. 3: Smoothed calibration curves for the baseline MLP model and its probabilistic variants in the METABRIC dataset. Left: observed versus predicted probability of event at four percentiles (25th, 50th, 75th and 90th) of the survival time. Right: kernel density plot visualizing the distribution of the predicted survival probabilities in the dataset.

almost perfectly calibrated in all scenarios, but has worse predictive performance than the Bayesian models.

- MCD offers a cheap way to give uncertainty estimates that can seem reasonable for some applications without having to double the number of model parameters, as VI mandates. However, a rigorous evaluation of its confidence intervals around the survival curve is needed to justify the quality of the approximation. To this end, we see a relatively small MAE, good C-calibration, but poor D-calibration in the SUPPORT and MIMIC-IV datasets.

Our work is important because, for the first time, it explicitly compares the extent to which different Bayesian approximation techniques using deep learning differ from each other and improves the prediction over traditional non-probabilistic alternatives. Future research may extend this work towards the direction of the latest machine learning research in probabilistic learning, such as conformal prediction, or recent frameworks that do not assume proportional hazards.

CONFLICT OF INTERESTS

The authors declare that they have no known conflict of interests or personal relationships that could have appeared to influence the work reported in this paper.

APPENDIX I PERFORMANCE METRICS

CI_{td}: The time-dependent concordance index determines if observations i, j are ranked concordantly by their predicted survival times [52]. In this sense, the ranking between i, j as the ranking between $S(T_i|\mathbf{x}_i(t))$ and $S(T_j|\mathbf{x}_j(t))$, if the survival functions are separated over the event horizon. If $S(T_i|\mathbf{x}_i(t)) < S(T_j|\mathbf{x}_j(t))$ for any t , then i has a predicted time lower than j . The CI_{td} is defined as [52]:

$$C_{td} = P(S(T_i|\mathbf{x}_i(t)) < S(T_i|\mathbf{x}_j(t)) \mid T_i < T_j \ \& \ \delta_i = 1) \quad (15)$$

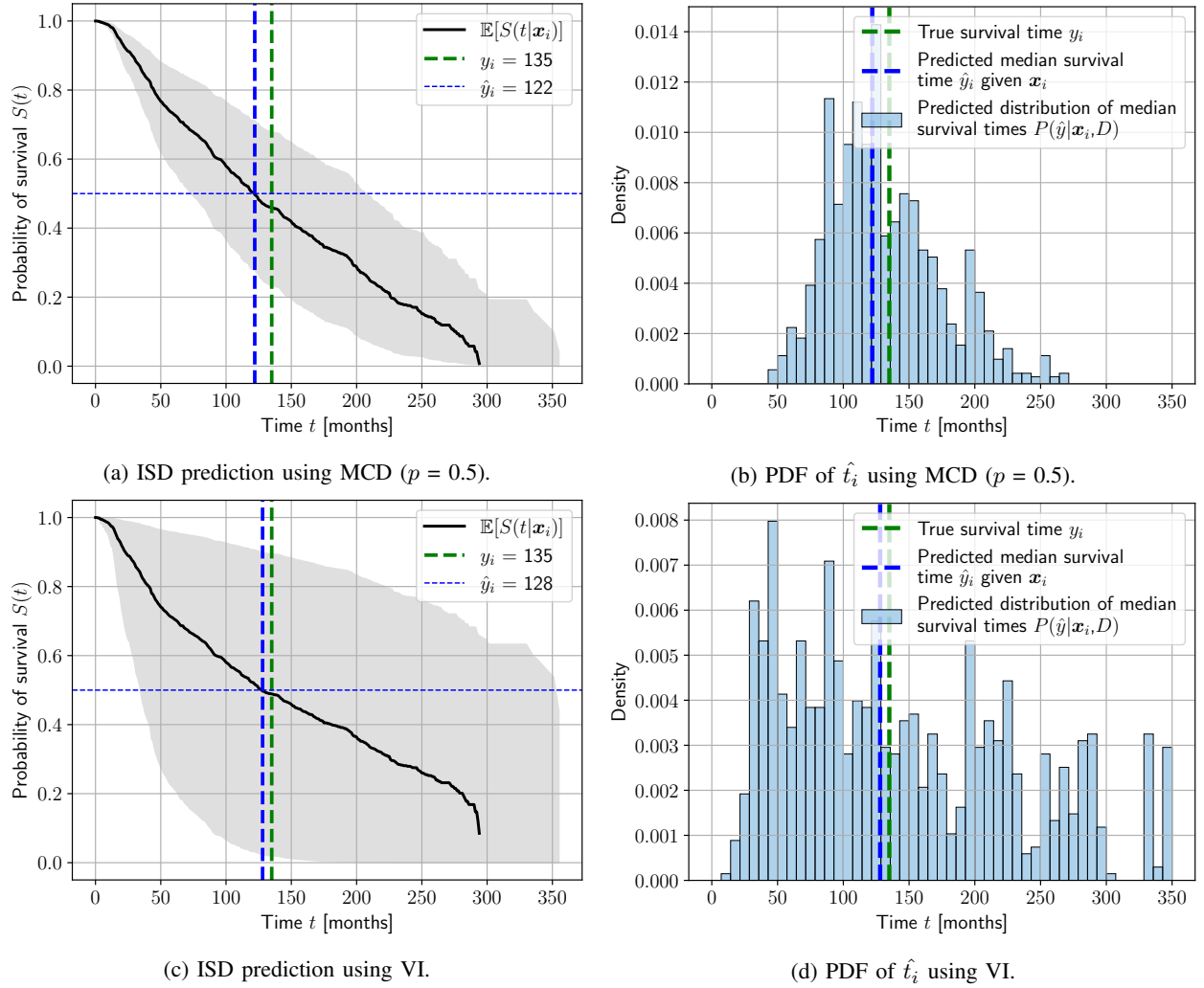


Fig. 4: Model prediction in the METABRIC dataset using the VI and MCD model on a randomly selected sample from the test set. The prediction is made by drawing 1000 samples from the predictive distribution. Left column: prediction of the individual survival distribution (ISD) and the associated 90% credible interval (shaded region) with the observed event time. The solid black curve is the mean ISD, and the surrounding CrIs represent the uncertainty in the prediction. The predicted event time is the median of the survival curve (the cross point of the black curve and the vertical blue dashed line). Right column: probability density function of the predicted median survival times. Although the VI model makes a better prediction of the survival time ($\hat{y}_i = 128$) than MCD ($\hat{y}_i = 122$), the variance in its prediction is significantly higher. This shows the importance of communicating the underlying variance when making a prediction, even when the model provides a satisfactory answer on average.

IBS: The Integrated Brier Score is the expectation of single-time Brier scores (BS) [54] over some interval $[t_k, t_K]$, where t_k denotes some measurement time on some discretized event horizon of K bins, $[t_0, t_1, t_2, \dots, t_K]$. The BS is the mean squared error between the observed binary outcome $y_i(t_k)$ and the predicted probability of the outcome $\hat{y}_i(t_k)$ at t_k . The metric has a probabilistic outcome constrained between zero and one, and the summation of all outcomes for a single individual must equal one. If we consider the entire event horizon $[t_0, t_K]$, then the IBS is defined as [54]:

$$IBS = \frac{1}{K} \sum_{t=0}^K \frac{1}{N} \sum_{i=1}^N (\hat{y}_i(t_k) - y_i(t_k))^2 \quad (16)$$

MAE: The mean absolute error is the absolute difference between the predicted and actual survival times. As proposed by [59], we use the median of the survival curve as the expected survival time. Given an individual survival distribution, $S(t | x_i) = P(T > t | x_i)$, we compute the predicted survival time \hat{y}_i as the median survival time [53]:

$$\hat{y}_i = \text{median}(S(t | x_i)) = S^{-1}(0.5 | x_i) \quad (17)$$

In this work, we report MAE_H and MAE_{PO} . The MAE_H uses a Hinge loss function to calculate the mean absolute error for censored individuals: if the predicted survival time is smaller than the time of censoring, the loss is the time of censoring minus the predicted time. If the predicted survival

time is equal to or greater than the time of censoring, the loss is zero. MAE_{PO} employs pseudo-observation to estimate the actual time of survival for censored individuals. For further details on MAE, see [53].

ICI: The Integrated Calibration Index is the absolute difference on average between the observed and predicted probabilities of event [55]. Adopting the notation of Austin and Steyerberg, let $f(x) = |x - x_c|$ denote the absolute difference between the calibration curve and the diagonal line of perfect calibration, where x is a predicted probability in the interval $[0, 1]$ and x_c is the value of the calibration curve at x . Let $\phi(x)$ denote the density function of the predicted probabilities distribution. The ICI is then a weighted average of the absolute differences between the calibration curve and the diagonal line of perfect calibration: $\text{ICI} = \int_0^1 f(x)\phi(x) dx$.

D-calibration: Distribution calibration measures the calibration performance of the survival curve $S(t)$ [56], expressing to what extent the predicted probabilities can be trusted. For any probability interval $[a, b] \in [0, 1]$, we define $D_m(a, b)$ as the subset of individuals in the dataset D whose predicted probability of event is in the interval $[a, b]$ [59]. A model is D-calibrated if the proportion of individuals $\frac{|D_m(a, b)|}{|D|}$ is statistically similar to the proportion $b - a$. We use a Pearson's χ^2 test to check if the proportion of events in each interval is uniformly distributed within mutually exclusive and equal-sized intervals, as proposed by [56]. As an obvious test for calibration, examine a group of individuals and determine the number who died before the median. If the survival curve is D-calibrated, approximately 50% of these individuals should die prior to their common predicted median survival time, and similarly, around 75% of individuals should be alive at the 25th percentile, and so on.

C-calibration: Coverage calibration is a statistical test to measure the agreement between the upper and lower bounds of the predicted credible intervals (CrIs) and the observed probability intervals [14]. For example, a 90% CrI should cover an individual's likelihood of an event with a probability of 90%. In practice, we calculate the observed coverage rates using CrIs with different percentages (ranging from 10% to 90%) and then use a Pearson's χ^2 test to evaluate the calibration of expected and observed coverage rates.

APPENDIX II HYPERPARAMETER OPTIMIZATION

The hyperparameters of the network include: the optimizer algorithm, the learning rate decay, the activation function, the batch size, the depth and size of the network, the learning rate, the ℓ_2 regularization coefficient, and the dropout rate. We use Bayesian optimization [51] to tune the hyperparameters of the respective models over ten iterations on the validation set. We use the hyperparameters leading to the highest concordance index (Antolini's). Note that for the MCD architecture, we manually set the dropout rate in each experiment. Table III reports the best-obtained hyperparameters for the respective models used in this work.

TABLE III: Selected hyperparameters for the proposed neural networks.

Hyperparameter	METABRIC	SEER	SUPPORT	MIMIC-IV
Optimizer	Adam	Adam	Adam	Adam
Decay	None	None	0.001	0.0001
Activation fn	ReLU	ReLU	ReLU	ReLU
Batch size	32	32	32	128
# Nodes/layer	[64, 128]	[64]	[128]	[32]
Learning rate	5e-3	1e-3	1e-3	1e-4
Activity ℓ_2 Reg	0.001	0.001	0.001	0.001
Dropout	0.25	0.25	0.25	0.5

- [1] H. Jiang, B. Kim, M. Guan, and M. Gupta, "To trust or not to trust a classifier," in *Advances in Neural Information Processing Systems*, vol. 31, 2018, pp. 5546–5557.
- [2] Y. Gal and Z. Ghahramani, "Dropout as a bayesian approximation: Representing model uncertainty in deep learning," in *Proceedings of The 33rd International Conference on Machine Learning*, vol. 48, 2016, pp. 1050–1059.
- [3] E. Hüllermeier and W. Waegeman, "Aleatoric and epistemic uncertainty in machine learning: an introduction to concepts and methods," *Machine Learning*, vol. 110, no. 3, pp. 457–506, 2021.
- [4] M. Magris and A. Iosifidis, "Bayesian learning for neural networks: an algorithmic survey," *Artificial Intelligence Review*, pp. 1–51, 2023.
- [5] A. Kendall and Y. Gal, "What uncertainties do we need in bayesian deep learning for computer vision?" in *Advances in Neural Information Processing Systems*, vol. 30, 2017.
- [6] D. R. Cox, "Regression models and life-tables," *Journal of the Royal Statistical Society: Series B (Methodological)*, vol. 34, no. 2, pp. 187–202, 1972.
- [7] D. W. Kim, S. Lee, S. Kwon, W. Nam, I.-H. Cha, and H. J. Kim, "Deep learning-based survival prediction of oral cancer patients," *Scientific Reports*, vol. 9, no. 1, p. 6994, 2019.
- [8] E. Giunchiglia, A. Nemchenko, and M. van der Schaar, "RNN-SURV: A Deep Recurrent Model for Survival Analysis," in *Artificial Neural Networks and Machine Learning – ICANN 2018*, vol. 11141, 2018, pp. 23–32.
- [9] J. Katzman, U. Shaham, J. Bates, A. Cloninger, T. Jiang, and Y. Kluger, "DeepSurv: personalized treatment recommender system using a cox proportional hazards deep neural network," *BMC Medical Research Methodology*, vol. 18, no. 1, 2018.
- [10] M. F. Gensheimer and B. Narasimhan, "A scalable discrete-time survival model for neural networks," *PeerJ*, vol. 7, pp. 1–17, 2019.
- [11] L. Zhao and D. Feng, "Deep Neural Networks for Survival Analysis Using Pseudo Values," *IEEE Journal of Biomedical and Health Informatics*, vol. 24, no. 11, pp. 3308–3314, 2020.
- [12] L. Zhao, "Deep neural networks for predicting restricted mean survival times," *Bioinformatics*, vol. 36, no. 24, pp. 5672–5677, 2021.
- [13] C. M. Lillelund, M. Magris, and C. F. Pedersen, "Uncertainty estimation in deep bayesian survival models," in *2023 IEEE EMBS International Conference on Biomedical and Health Informatics (BHI)*, 2023, pp. 1–4.
- [14] S.-a. Qi, N. Kumar, R. Verma, J.-Y. Xu, G. Shen-Tu, and R. Greiner, "Using bayesian neural networks to select features and compute credible intervals for personalized survival prediction," *IEEE Transactions on Biomedical Engineering*, vol. 70, no. 12, pp. 3389–3400, 2023.
- [15] H. Loya, P. Poduval, D. Anand, N. Kumar, and A. Sethi, "Uncertainty estimation in cancer survival prediction," Accepted at AI4AH Workshop at ICLR 2020, 2020.
- [16] A. G. Roy, S. Conjeti, N. Navab, and C. Wachinger, "Bayesian quicknat: Model uncertainty in deep whole-brain segmentation for structure-wise quality control," *NeuroImage*, vol. 195, pp. 11–22, 2019.
- [17] J. Lee, J. Feng, M. Humt, M. G. Müller, and R. Triebel, "Trust your robots! predictive uncertainty estimation of neural networks with sparse gaussian processes," in *Conference on Robot Learning*, 2022, pp. 1168–1179.
- [18] Y. Ovadia, E. Fertig, J. Ren, Z. Nado, D. Sculley, S. Nowozin, J. Dillon, B. Lakshminarayanan, and J. Snoek, "Can you trust your model's uncertainty? evaluating predictive uncertainty under dataset shift," in *Advances in Neural Information Processing Systems*, vol. 32, 2019, p. 14003–14014.

- [19] A. G. Wilson and P. Izmailov, "Bayesian deep learning and a probabilistic perspective of generalization," in *Advances in Neural Information Processing Systems*, vol. 33, 2020, pp. 4697–4708.
- [20] C. Blundell, J. Cornebise, K. Kavukcuoglu, and D. Wierstra, "Weight uncertainty in neural networks," in *Advances in Neural Information Processing Systems*, vol. 37, 2015, p. 1613–1622.
- [21] B. He and S. Luo, "Joint modeling of multivariate longitudinal measurements and survival data with applications to parkinson's disease," *Statistical Methods in Medical Research*, vol. 25, no. 4, pp. 1346–1358, 2016.
- [22] V. G. Hennessey, L. G. Leon-Novelo, J. Li, L. Zhu, E. Chi, and J. G. Ibrahim, "A bayesian joint model for longitudinal das28 scores and competing risk informative drop out in a rheumatoid arthritis clinical trial," *arXiv:1801.08628*, 2018.
- [23] H. Zhu, S. M. DeSantis, and S. Luo, "Joint modeling of longitudinal zero-inflated count and time-to-event data: A bayesian perspective," *Statistical Methods in Medical Research*, vol. 27, no. 4, pp. 1258–1270, 2018.
- [24] S. Sinharay, "Experiences with markov chain monte carlo convergence assessment in two psychometric examples," *Journal of Educational and Behavioral Statistics*, vol. 29, no. 4, pp. 461–488, 2004.
- [25] A. Graves, "Practical variational inference for neural networks," in *Advances in Neural Information Processing Systems*, vol. 24, 2011.
- [26] J. Liu, Z. Lin, S. Padhy, D. Tran, T. Bedrax Weiss, and B. Lakshminarayanan, "Simple and principled uncertainty estimation with deterministic deep learning via distance awareness," in *Advances in Neural Information Processing Systems*, vol. 33, 2020, pp. 7498–7512.
- [27] I. Osband, C. Blundell, A. Pritzel, and B. V. Roy, "Deep exploration via bootstrapped dqn," in *Advances in Neural Information Processing Systems*, vol. 29, 2016.
- [28] T. Pearce, N. Anastassacos, M. Zaki, and A. Neely, "Bayesian inference with anchored ensembles of neural networks, and application to exploration in reinforcement learning," Published at the Exploration in Reinforcement Learning Work- shop at the 35th International Conference on Machine Learning, 2018.
- [29] J. Caldeira and B. Nord, "Deeply uncertain: comparing methods of uncertainty quantification in deep learning algorithms," *Machine Learning: Science and Technology*, vol. 2, no. 1, p. 015002, 2020.
- [30] S. Boluki, R. Ardywibowo, S. Z. Dadaneh, M. Zhou, and X. Qian, "Learnable bernoulli dropout for bayesian deep learning," in *Proceedings of the 23rd International Conference on Artificial Intelligence and Statistics (AISTATS)*, vol. 37, 2020.
- [31] F. Verdoja and V. Kyrki, "Notes on the behavior of mc dropout," Presented at the ICML 2021 Workshop on "Uncertainty and Robustness in Deep Learning", 2021.
- [32] J. G. Ibrahim, M.-H. Chen, and D. Sinha, *Bayesian Survival Analysis*. Springer-Verlag, 2001.
- [33] D. Alvares, E. Lázaro, V. Gómez-Rubio, and C. Armero, "Bayesian survival analysis with bugs," *Statistics in Medicine*, vol. 40, no. 12, pp. 2975–3020, 2021.
- [34] R. Li, C. Chang, J. M. Justesen, Y. Tanigawa, J. Qian, T. Hastie, M. A. Rivas, and R. Tibshirani, "Fast Lasso method for large-scale and ultrahigh-dimensional Cox model with applications to UK Biobank," *Biostatistics*, vol. 23, no. 2, pp. 522–540, 2020.
- [35] Z. Zhang, A. Stringer, P. Brown, and J. Stafford, "Bayesian inference for cox proportional hazard models with partial likelihoods, nonlinear covariate effects and correlated observations," *Statistical Methods in Medical Research*, vol. 32, no. 1, pp. 165–180, 2023.
- [36] C. Nagpal, X. Li, and A. Dubrawski, "Deep survival machines: Fully parametric survival regression and representation learning for censored data with competing risks," *IEEE Journal of Biomedical and Health Informatics*, vol. 25, no. 8, 2021.
- [37] C.-N. Yu, R. Greiner, H.-C. Lin, and V. Baracos, "Learning patient-specific cancer survival distributions as a sequence of dependent regressors," in *Advances in Neural Information Processing Systems*, vol. 24, 2011.
- [38] J. Gareth, W. Daniela, H. Trevor, and T. Robert, *An introduction to statistical learning: with applications in R*, 2nd ed. Springer, 2021.
- [39] E. L. Kaplan and P. Meier, "Nonparametric estimation from incomplete observations," *Journal of the American Statistical Association*, vol. 53, no. 282, pp. 457–481, 1958.
- [40] Y. Gal, "Uncertainty in deep learning," Ph.D. dissertation, University of Cambridge, 2016.
- [41] J. Liu, Z. Lin, S. Padhy, D. Tran, T. Bedrax Weiss, and B. Lakshminarayanan, "Simple and principled uncertainty estimation with deterministic deep learning via distance awareness," *Advances in Neural Information Processing Systems*, vol. 33, pp. 7498–7512, 2020.
- [42] C. Lee, W. Zame, J. Yoon, and M. Van Der Schaar, "Deephit: A deep learning approach to survival analysis with competing risks," *Proceedings of the AAAI Conference on Artificial Intelligence*, vol. 32, no. 1, 2018.
- [43] METABRIC Group, C. Curtis, S. P. Shah, S.-F. Chin, G. Turashvili, O. M. Rueda, M. J. Dunning, D. Speed, A. G. Lynch, S. Samarajiwa, Y. Yuan, S. Gräf, G. Ha, G. Haffari, A. Bashashati, R. Russell, S. McKinney, A. Langerød, A. Green, E. Provenzano, G. Wishart, S. Pinder, P. Watson, F. Markowitz, L. Murphy, I. Ellis, A. Purushotham, A.-L. Børresen-Dale, J. D. Brenton, S. Tavaré, C. Caldas, and S. Aparicio, "The genomic and transcriptomic architecture of 2,000 breast tumours reveals novel subgroups," *Nature*, vol. 486, no. 7403, pp. 346–352, 2012.
- [44] L. A. Gloeckler Ries, M. E. Reichman, D. R. Lewis, B. F. Hankey, and B. K. Edwards, "Cancer survival and incidence from the surveillance, epidemiology, and end results (SEER) program," *Oncologist*, vol. 8, no. 6, pp. 541–552, 2003.
- [45] W. A. Knaus, "The support prognostic model: Objective estimates of survival for seriously ill hospitalized adults," *Annals of Internal Medicine*, vol. 122, no. 3, pp. 191–203, 1995.
- [46] A. E. W. Johnson, L. Bulgarelli, L. Shen, A. Gayles, A. Shammout, S. Horng, T. J. Pollard, S. Hao, B. Moody, B. Gow, L.-w. H. Lehman, L. A. Celi, and R. G. Mark, "MIMIC-IV, a freely accessible electronic health record dataset," *Scientific Data*, vol. 10, no. 1, p. 1, 2023.
- [47] N. Simon, J. Friedman, T. Hastie, and R. Tibshirani, "Regularization paths for cox's proportional hazards model via coordinate descent," *Journal of statistical software*, vol. 39, no. 5, pp. 1–13, 2011.
- [48] J. H. Friedman, "Greedy function approximation: A gradient boosting machine," *The Annals of Statistics*, vol. 29, no. 5, pp. 1189–1232, 2001.
- [49] H. Ishwaran, U. B. Kogalur, E. H. Blackstone, and M. S. Lauer, "Random survival forests," *The Annals of Applied Statistics*, vol. 2, no. 3, pp. 841–860, 2008.
- [50] C. Nagpal, S. Yadlowsky, N. Rostamzadeh, and K. Heller, "Deep Cox Mixtures for Survival Regression," in *Proceedings of Machine Learning Research*, vol. 126, 2021, pp. 1–27.
- [51] J. Snoek, H. Larochelle, and R. P. Adams, "Practical bayesian optimization of machine learning algorithms," in *Advances in Neural Information Processing Systems*, vol. 25, 2012.
- [52] L. Antolini, P. Boracchi, and E. Biganzoli, "A time-dependent discrimination index for survival data," *Statistics in Medicine*, vol. 24, no. 24, pp. 3927–3944, 2005.
- [53] S.-a. Qi, W. Sun, and R. Greiner, "SurvivalEVAL: A comprehensive open-source python package for evaluating individual survival distributions," *Proceedings of the AAAI Symposium Series*, vol. 2, pp. 453–457, 2024.
- [54] E. Graf, C. Schmoor, W. Sauerbrei, and M. Schumacher, "Assessment and comparison of prognostic classification schemes for survival data," *Statistics in Medicine*, vol. 18, no. 17-18, pp. 2529–2545, 1999.
- [55] P. C. Austin and E. W. Steyerberg, "The integrated calibration index (ici) and related metrics for quantifying the calibration of logistic regression models," *Statistics in Medicine*, vol. 38, no. 21, pp. 4051–4065, 2019.
- [56] H. Haider, B. Hoehn, S. Davis, and R. Greiner, "Effective ways to build and evaluate individual survival distributions," *Journal of Machine Learning Research*, vol. 21, no. 1, pp. 1–63, 2020.
- [57] T. Hothorn, P. Bühlmann, S. Dudoit, A. Molinaro, and M. J. Van Der Laan, "Survival ensembles," *Biostatistics*, vol. 7, no. 3, pp. 355–373, 2005.
- [58] H. Steck, B. Krishnapuram, C. Dehing-oberije, P. Lambin, and V. C. Raykar, "On ranking in survival analysis: Bounds on the concordance index," in *Advances in Neural Information Processing Systems*, vol. 20, 2007.
- [59] S. Qi, N. Kumar, M. Farrokh, W. Sun, L. Kuan, R. Ranganath, R. Henao, and R. Greiner, "An effective meaningful way to evaluate survival models," *Proceedings of Machine Learning Research*, vol. 202, pp. 28 244–28 276, 2023.